

Fig. 3 Experiments of leading edge.

The radius of the blunted nose was less than about 0.05 cm in diameter, that is, Reynolds number was about  $10^5$ . The measurements were carried out at the position of 120 mm from the nose, as shown in Fig. 1. According to Chernyi,<sup>8</sup> a flow pattern around a slightly blunted cone becomes almost the same as a pointed cone, in the case that bluntness factor  $\sqrt{2/C_D} \cdot x/d \cdot \tan^2 \beta$  is larger than about 1.5, where  $C_D$ ,  $x$ ,  $d$ , and  $\beta$  are the drag coefficient, distance from the nose, radius of the blunted nose, and semiapex angle of the nose, respectively. If the theory can be applied to our case, the flow pattern in this experiment may be considered to be a conical flow since the bluntness factor is about 70.

Figure 2 showed the experimental results for the angles of attack  $\alpha = 0, 10, 20$ , and  $30$  deg. Double shock patterns, which consisted of a wing shock and a body shock, occurred in cases of  $\alpha = 0$  and  $10$  deg. On the other hand, single shock patterns, compounded by a wing shock and a body shock, appeared in cases of  $\alpha = 20$  and  $30$  deg. The results of the double shock patterns agreed well with those obtained by the vapor screen method.<sup>6</sup>

More precise experiments near the wing leading edge were carried out in cases of  $\alpha = 21, 22$ , and  $23$  deg, and the results were shown in Fig. 3. At  $\alpha = 21$  deg, the shock wave was attached at the leading edge, while it was detached from the leading edge at  $\alpha = 22$  and  $23$  deg. This agreed approximately with the result of Ref. 9.

At  $\alpha = 0$  or  $10$  deg, it was impossible to observe the corner shock wave by an optical system, since light paths were prevented from passing through by the wing or the body. The electric discharge method is superior to any optical method in this respect.

## References

- Weinstein, L. M., Wagner, R. D., Jr., and Ocheltree, S. L., "Electron Beam Flow Visualization in Hypersonic Helium Flow," *AIAA Journal*, Vol. 6, Aug. 1968, pp. 1023-1025.
- Muntzs, E. P. and Marsden, D. J., *Investigation of Flows with Electron Beam*, pp. 495-526.
- Rothe, D. E., "Flow Visualization Using a Traversing Electron Beam," *AIAA Journal*, Vol. 3, Oct. 1965, pp. 1945-1946.
- Maguire, B. L., Mallin, J. R., and Muntzs, E. P., "Visualization Technique for Low-Density Flow Fields," *IEEE Transactions*, Vol. AES-3, No. 2, 1967, pp. 321-326.
- Rao, D. M., "Delta Wing Shock Shape at Hypersonic Speed," *AIAA Journal*, Vol. 9, Oct. 1971, pp. 2093-2094.
- Scheuing, R. A., "Outer Inviscid Hypersonic Flow with Attached Shock Waves," *ARS Journal*, April 1961, pp. 486-505.
- Kimura, T., Nishio, M., Fujita, T., and Maeno, "Visualization of Shock Wave by Electric Discharge," *AIAA Journal*, Vol. 15, May 1977, pp. 611-612.
- Chernyi, G. G., *Introduction to Hypersonic Flow*, Academic Press, New York, 1961, pp. 226-231.
- Goebel, T. P., Martin, J. J., and Boyd, J. A., "Factors Affecting Lift-Drag Ratios at Mach Numbers from 5 to 20," *AIAA Journal*, Vol. 1, March 1963, pp. 640-650.

J80-158

## Analysis of the Strong Interaction Problem with Slip and Temperature-Jump Effects

20013

20017

R. N. Gupta\* and S. Menon†

Indian Institute of Technology, Kanpur, India  
and

C. M. Rodkiewicz‡

University of Alberta, Edmonton, Canada

## Introduction

THE analysis of the hypersonic interaction problem without slip and temperature-jump conditions on a flat plate by utilizing the boundary-layer equations is well documented.<sup>1,2</sup> For the interaction problem with slip and temperature-jump effects, Ref. 3 has provided a solution which is an expansion in terms of the slip parameter about the no-slip strong interaction solution. Analysis of Ref. 3, however, would be more appropriate for the cold wall case where the slip and temperature-jump effects are much smaller. The momentum integral-equation formulation of Ref. 4 suffers from the fact that the use of a linear velocity profile does not allow a complete accounting of the viscous effects in the momentum equation. Further, in this approach the integrator is started right from  $x=0$ , thus covering the noncontinuum flow and continuum-merged flow regimes where the boundary layer equations cannot, strictly speaking, be used. In the present analysis, a finite-difference solution to the strong interaction problem with slip and temperature-jump effects is given by utilizing the boundary layer equations.

## Flow Equations and Discussion of Results

Under the assumption of a linear viscosity relation of the form  $\mu = CT$ , the transformed boundary-layer momentum and energy equations may be written in terms of the dimensionless stream function  $f$  and the dimensionless total enthalpy  $H$  as<sup>2</sup>

$$\begin{aligned} \bar{p} \frac{\partial^3 f}{\partial \eta^3} + f \frac{\partial^2 f}{\partial \eta^2} - 4x \left( \frac{\partial f}{\partial \eta} \frac{\partial^2 f}{\partial x \partial \eta} - \frac{\partial f}{\partial x} \frac{\partial^2 f}{\partial \eta^2} \right) \\ = \left( \frac{\gamma-1}{\gamma} \right) \left( \frac{2x}{\bar{p}} \frac{d\bar{p}}{dx} - 1 \right) \left[ H - \left( \frac{\partial f}{\partial \eta} \right)^2 \right] \end{aligned} \quad (1)$$

$$\begin{aligned} \frac{\bar{p}}{Pr} \frac{\partial^2 H}{\partial \eta^2} + f \frac{\partial H}{\partial \eta} - 4x \left( \frac{\partial f}{\partial \eta} \frac{\partial H}{\partial x} - \frac{\partial f}{\partial x} \frac{\partial H}{\partial \eta} \right) \\ = \frac{2(1-Pr)}{Pr} \bar{p} \left[ \left( \frac{\partial^2 f}{\partial \eta^2} \right)^2 + \frac{\partial f}{\partial \eta} \frac{\partial^3 f}{\partial \eta^3} \right] \end{aligned} \quad (2)$$

In order to bring out the character of strong interaction solutions as distinct from weak interactions, pressure has been retained as a coefficient of higher order terms in Eqs. (1) and

Received June 20, 1979; revision received Nov. 15, 1979. Copyright © American Institute of Aeronautics and Astronautics, Inc., 1979. All rights reserved.

Index categories: Rarefied Flows; Supersonic and Hypersonic Flow. \*Professor, Dept. of Aeronautical Engineering. Member AIAA.

†Presently, Dept. of Aerospace Engineering, University of Maryland.

‡Professor of Mechanical Engineering.

In fond memory of M. H. Bertram with whom one of us (RNG) spent many fruitful years.

(2). The normalized value  $\bar{p}$  of the pressure has been obtained from the tangent-wedge equation:<sup>1,2</sup>

$$\bar{p}(x) = \frac{p}{p_0 \chi} = \frac{1}{p_0 \chi} \left[ 1 + \gamma K \left\{ \frac{\gamma+1}{4} K + \left[ \left( \frac{\gamma+1}{4} K \right)^2 + 1 \right]^{1/2} \right\} \right] \quad (3)$$

with

$$K(x) = M_\infty \frac{d\delta}{dx} \quad (4)$$

and

$$\delta(x) = \frac{\delta^*}{L^*} = \frac{(\gamma-1)}{p_0^{1/2}} \frac{\chi L^*}{M_\infty} \frac{x^{3/4}}{\bar{p}} \int_0^\infty \left[ H - \left( \frac{\partial f}{\partial \eta} \right)^2 \right] d\eta \quad (5)$$

where  $M_\infty$  is the freestream Mach number,  $\delta^*$  is the boundary layer displacement thickness and  $\chi$  is the hypersonic interaction parameter.

The boundary conditions associated with the problem are: without slip at wall (i.e., at  $\eta=0$ ),  $f = \partial f / \partial \eta = \partial H / \partial \eta = 0$ , or  $H = H_w = \text{const.}$ ; and with slip at  $\eta=0^+$ ,  $\partial f / \partial \eta = \epsilon \partial^2 f / \partial \eta^2$ ,  $f = \partial H / \partial \eta = 0$  or  $H = H_w + (B/A) \epsilon (\partial H / \partial \eta) + \text{terms of order } \epsilon^2$ . Here  $\eta=0^+$  denotes the bottom of the continuum gas layer next to the wall and  $\epsilon$  is the slip parameter defined as:<sup>3</sup>

$$\epsilon = A [ (\pi \gamma) (\gamma-1) / 16 p_0 ]^{1/2} H_w^{1/2} \bar{V}_\infty^{1/2} \quad (6)$$

where the constants  $A$  and  $B$  are obtained from kinetic flow considerations. At the edge of the boundary layer (i.e., at  $\eta \rightarrow \infty$ ),  $\partial f / \partial \eta = H = 1$ , where terms of order  $M_\infty^{-2}$  have been neglected.

For the no-slip case, the finite-difference solution is started at some initial line  $x=x_i$  by utilizing the series solution of Ref. 4. Here  $x_i$  corresponds to  $\chi \sim 0$  (100). The interaction between the boundary layer and the external flow field has been analyzed by a two-step iteration cycle: In the first step, Eqs. (1) and (2) are solved for any given  $\bar{p}(x)$  distribution in the region  $x_i \leq x \leq 1$ ,  $0 \leq \eta \leq \eta_\delta$  subject to the initial and boundary conditions; next, a new  $\bar{p}(x)$  distribution is obtained from the solutions  $f(x, \eta)$  and  $H(x, \eta)$  provided by the first step. These two steps are repeated until  $\bar{p}(x)$  converges within a specified tolerance. The numerical solution to Eqs. (1) and (2) has been obtained by the "difference-differential" technique developed by Clutter and Smith<sup>5</sup> by incorporating the appropriate changes. Since these equations are iterated with the full tangent-wedge inviscid approximation, one is able to integrate them continuously from the strong interaction zone to the weak interaction region.

For the slip case, the two-step iteration cycle is started by using the results of the no-slip series solution to determine the initial  $x$ -wise gradients of the variables by taking forward finite differences along the entire length of the plate. In the second step the new  $\bar{p}(x)$  is calculated by utilizing the solutions of the first step, and also the new  $x$ -wise gradients of the flow variables (with the inclusion of slip effects) are estimated by the forward difference formulation. These new computed gradients at each station (including the initial one) are successively updated towards the final slip values. The above two-step cycle is continued until  $|\bar{p}^{i+1} - \bar{p}^i| / \bar{p}^i < \epsilon_i$  where  $\epsilon_i$  is a small number of the order of  $10^{-3}$  and  $i$  is the iteration cycle number.

Figure 1 compares the present induced pressure results for an insulated and cooled surface with the available experimental data. For the insulated case given in Fig. 1a, there is a good agreement with Bertram's data<sup>1,6</sup> downstream along the plate. However, the agreement with the experimental data of Moulic and Maslach<sup>7</sup> and Chuan and Waiter<sup>8</sup> is somewhat poor. The theoretical estimates of Aroesty<sup>3</sup> and Kumar and Jain<sup>4</sup> are somewhat higher in the upstream region (where the slip effects are maximum) as compared to the present computations. For the cooled surface, the present predictions fall within range of the experimental scatter<sup>9,10</sup> and quite good agreement is noted with the data of Ref. 11 for  $T_w/T_0 = 0.15$  as shown in Fig. 1b. The beginning of a pressure plateau is also noticeable in this figure. The present results, computed by using the boundary layer equations, should not be taken seriously beyond a value of the rarefaction parameter  $\bar{V}_\infty$  approximately equal to 0.3. Figure 1b also contains the strong interaction theory results of Cheng et al.<sup>12</sup>

Figures 2 and 3 give the variations of skin friction coefficient  $C_f$  and Stanton number  $St$  for a cooled surface. For the strong interaction flow without slip,  $\bar{C}_f = M_\infty^3 C_f / 2 \chi^{3/2}$  has a constant value,<sup>2,13</sup> as shown in Fig. 2. The increase in  $C_f$  in the weak interaction limit and decrease in the low density limit are indicative of the departure from the strong interaction theory. Data of Vidal and Bartz<sup>14</sup> and Wallace and Burke<sup>15</sup> show similar trends though they are lower than the present results. The computations of Shorenstein and Probst<sup>13</sup> made for the viscous shock-layer regime show a better correlation with the experimental data of large  $\bar{V}_\infty$ . With the increase in Reynolds number (or decreasing  $\bar{V}_\infty$ ) their results seem to tend towards the present computations. As compared to the skin friction coefficient, the correlation between the present predictions of heat transfer at the wall and the

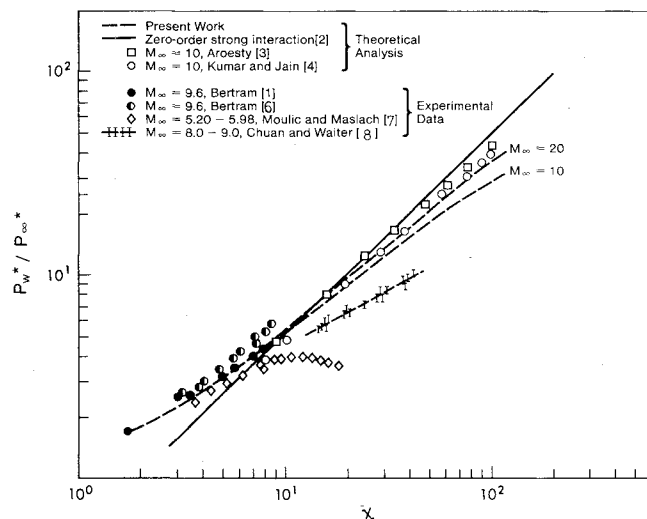


Fig. 1a Variation of surface pressure with interaction parameter for an insulated surface.

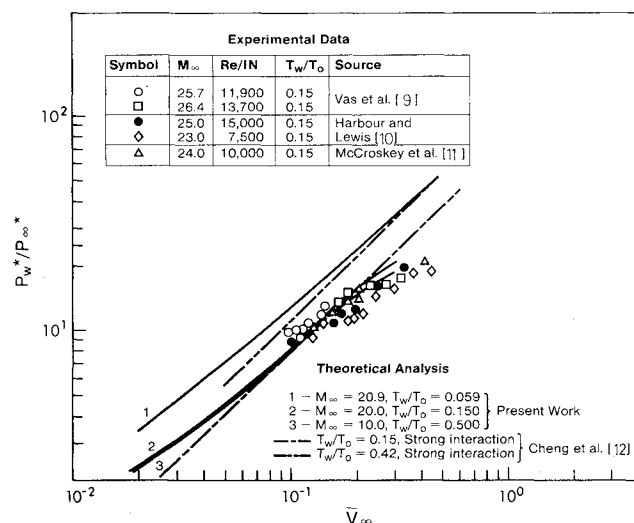


Fig. 1b Pressure distribution on a sharp flat plate as a function of rarefaction parameter (cooled surface).

<sup>3</sup>In Ref. 3, the factor  $(\pi \gamma)^{1/2}$  appears to have been left out in deriving the expression for  $\epsilon$ .

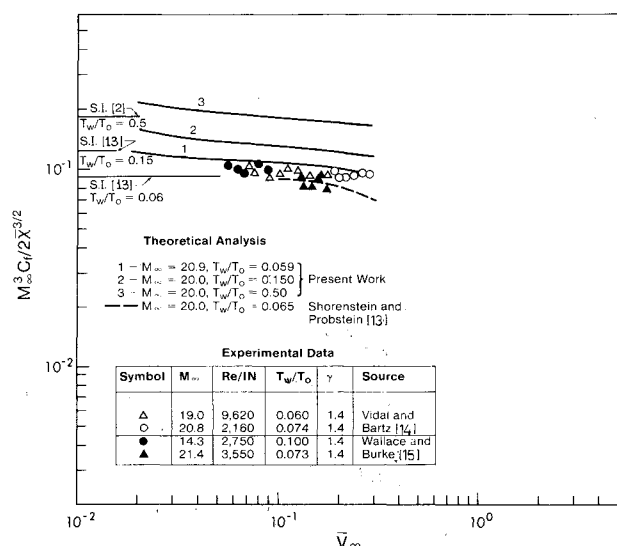


Fig. 2 Variation of skin friction on a sharp flat plate as a function of rarefaction parameter (cooled surface).

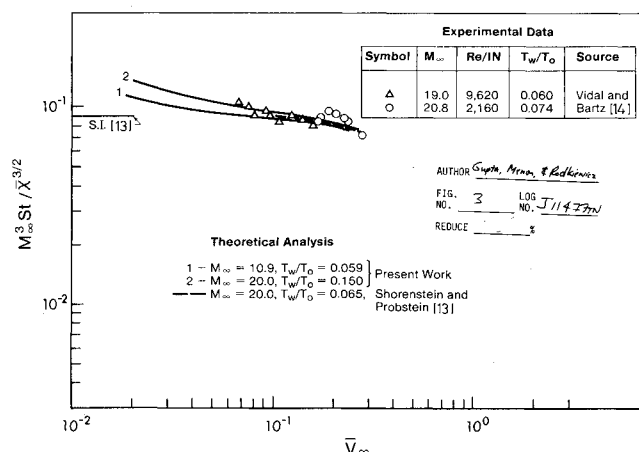


Fig. 3 Variation of Stanton number on a sharp flat plate as a function of rarefaction parameter (cooled surface).

measurements<sup>14</sup> is quite good, as shown in Fig. 3. As before, Shorenstein and Probst's analysis<sup>13</sup> tends towards the present results in the downstream limit. It may be seen from Figs. 2 and 3 that as the plate is progressively cooled, both skin friction and heat transfer decrease because of the lower viscosity and thermal conductivity values at the cooled surface.

Finally, the present analysis does give a picture of the flowfield in the region downstream of the viscous shock layer that is qualitatively correct (i.e., the tendency of the experimental data to level off at large values of  $\bar{\chi}$  is represented) and numerically accurate within the framework of the boundary layer theory.

## References

- Hays, W. D. and Probst, R. F., *Hypersonic Flow Theory*, Academic Press, New York, 1959.
- Chatopadhyay, T. K. and Rodkiewicz, C. M., "Hypersonic Strong Interaction Flow over an Inclined Surface," *AIAA Journal*, Vol. 9, March 1971, pp. 535-537.
- Aroesty, J., "Strong Interaction with Slip Boundary Conditions," University of California (Berkeley) Institute of Engineering Research, Tech. Rept. HE-150-188, 1961.
- Kumar, A. and Jain, A. C., "Hypersonic Viscous Slip Flow over Insulated Wedges," *AIAA Journal*, Vol. 10, Aug. 1972, pp. 1081-1083.
- Clutter, W. D. and Smith, A.M.O., "Solutions of the General Boundary Layer Equations for Compressible Laminar Flow Including

Transverse Curvature," *AIAA Journal*, Vol. 3, April 1965, pp. 639-647.

<sup>6</sup>Bertram, M. H., "Boundary Layer Displacement Effects in Air at Mach Numbers of 6.8 and 9.6," NASA TR R-22, 1959.

<sup>7</sup>Moulic, E. S. and Maslach, G. J., "Induced Pressure Measurements on a Sharp Edged Insulated Flat Plate in Low Density Hypersonic Flow," *Rarefied Gas Dynamics*, Vol. 2, Suppl. 4, Academic Press, New York, 1967, pp. 971-992.

<sup>8</sup>Chuan, R. L. and Waiter, S. A., "Experimental Study of Hypersonic Rarefied Gas Dynamics, Vol. 2, Suppl. 2, Academic Press, New York, 1963, pp. 328-342.

<sup>9</sup>Vas, I. E., McDougall, J., Koppenwallner, G., and Bogdonoff, S. M., "Some Exploratory Experimental Studies of Hypersonic Low Density Effects on Flat Plates and Cones," *Rarefied Gas Dynamics*, Vol. 1, Suppl. 3, Academic Press, New York, 1965, pp. 508-534.

<sup>10</sup>Harbour, P. J. and Lewis, S. H., "Preliminary Measurements of the Hypersonic Rarefied Flow Field on a Sharp Flat Plate Using an Electron Beam Probe," *Rarefied Gas Dynamics*, Vol. 2, Suppl. 4, Academic Press, New York, 1967, pp. 1031-1046.

<sup>11</sup>McCroskey, W. J., Bogdonoff, S. M., and McDougall, J. G., "An Experimental Model for the Sharp Flat Plate in Rarefied Hypersonic Flow," *AIAA Journal*, Vol. 4, Sept. 1966, pp. 1580-1587.

<sup>12</sup>Cheng, H. K., Hall, J. G., Golian, T. C., and Hertzberg, A., "Boundary Layer Displacement and Leading Edge Bluntness Effects in High Temperature Hypersonic Flow," *Journal of Aerospace Sciences*, Vol. 28, May 1961, pp. 353-381.

<sup>13</sup>Shorenstein, M. L. and Probst, R. F., "The Hypersonic Leading Edge Problem," AIAA Paper 68-4, 1968.

<sup>14</sup>Vidal, R. J. and Bartz, J. A., "Surface Measurements on Sharp-Flat Plates and Wedges in Low Density Hypersonic Flow," *AIAA Journal*, Vol. 7, June 1969, pp. 1099-1109.

<sup>15</sup>Wallace, J. E. and Burke, A. F., "An Experimental Study of Surface and Flow Field Effects in Hypersonic Low Density Flow over a Flat Plate," *Rarefied Gas Dynamics*, Vol. 1, Suppl. 3, Academic Press, New York, 1965, pp. 487-507.

## J80-159 Boundary Layer of Density-Stratified Fluids with a Suspension of Particles

20002

20008

20009

L. M. Srivastava,\* V. P. Srivastava,\*  
and R. P. Agarwal\*

Motilal Nehru Regional Engineering College,  
Allahabad, India

## Introduction

THE study of the fluid dynamics of a particulate suspension (where the suspended matter may consist of solid particles, liquid droplets, gas bubbles, etc.) is of interest in a wide range of areas of scientific and technical importance. The theoretical study of this system of fluids has been very useful in understanding such phenomena as sedimentation, fluidization, combustion, atmospheric fallout, electrostatic precipitation of dust, nuclear reactor cooling, flows in rocket tubes, lunar ash flows, environmental pollution, aerosol and paint spraying, aircraft icing, and, more recently, blood flow. The study of boundary layers of the flow of particulate suspensions is important in collecting much useful information, including information concerning particle accumulation, retardation, and impingement on solid surfaces. These studies include the work of Marble,<sup>1</sup> Chiu,<sup>2</sup> Singleton,<sup>3,4</sup> Soo,<sup>5</sup> and Zung.<sup>6</sup> Tabakoff and Hamed<sup>7</sup> analyzed boundary layers of particulate flow in cascades in detail using the momentum integral method. They found that the presence of particles leads to an increase in the gas

Received Aug. 7, 1979; revision received Oct. 29, 1979. Copyright © American Institute of Aeronautics and Astronautics, Inc., 1979. All rights reserved.

Index categories: Boundary Layers and Convective Heat Transfer—Laminar; Nonsteady Aerodynamics; Multiphase Flows.

\*Dept. of Applied Mathematics.